

CubeSat Radar Cross-Section Measurement Campaign Paper for AMOS Conference Proceedings

Matt Mayne
Dstl, UK MOD

ABSTRACT

A CubeSat Radar Cross-Section (RCS) Measurement campaign was conducted by Dstl, part of UK MOD, in support of UK Space Domain Awareness (SDA) research activities that aim to better understand satellite signatures. The measurement campaign involved assessing the RCS of a CubeSat in a UK-based measurement chamber. This opportunity to capture the RCS of a real satellite has provided important understanding of the RCS levels that might be expected from typical CubeSat targets. Measurements were made of both the Flight Model (FM) and a representative Engineering Model (EM) across a 3-40GHz frequency range, Horizontal and Vertical polarisations and at multiple orientations. In addition, a study on physical variations such as component deployment was carried out in order to produce a comprehensive dataset of the satellite.

Developing an understanding of the Radio Frequency (RF) signatures of satellites is key to improving SDA capabilities, as it allows for an appreciation of how different satellites may appear to an observing radar. A subset of FM measurements were used to validate a broader set of measurements conducted on the electromagnetic representative EM. The EM was built using a combination of FM spare parts and specifically procured and produced representative model components, allowing for a greatly expanded measurement list.

The data collected has been processed and analysed to highlight and extract relevant features and identify dominant sources of scatter on the satellite. Inverse Synthetic Aperture Radar (ISAR) imagery was produced from the results enabling the identification of the target's configuration and orientation at the time of measurement. Dstl's research into ISAR systems has been previously reported at AMOS [1]. This could allow for the identification of the orientation of a satellite on-orbit including any changes to that orientation between orbits. This ability could potentially contribute to the fulfilment of a number of the UK government's published SDA requirements, reported recently at AMOS [2] [3], particularly those related to object characterisation (UKSDA-SR-7300).

Once the CubeSat has been successfully launched and is on-orbit, it is planned to track the satellite and collect in-situ data. Opportunities are put forward for interested parties to become involved in this effort. This data will be used to provide corresponding orbital RCS measurement data to sit alongside both computer simulated data and the anechoic chamber RCS data collected in this campaign.

1. INTRODUCTION

An object's RCS is a useful measure for determining its degree of visibility to a radar system [4], and is dependent on a number of factors including the configuration and orientation of the satellite exposed to the radar at any given time. Understanding the RCS of a satellite can hence provide the observer with better situational awareness of the satellite's condition, and any changes in RCS can be analysed in an attempt to determine the source of this change; whether due to an on-orbit manoeuvre, changes in configuration, or damage from debris or other environmental factors. However, characterisation of a satellite's RCS prior to launch can prove challenging as it is difficult to replicate a protected clean room environment within typical RCS measurement facilities.

A CubeSat Radar Cross-Section (RCS) Measurement campaign (2023-2024) was conducted by Dstl, part of UK MOD, in support of UK Space Domain Awareness (SDA) research activities aiming to better understand satellite signatures. The measurement campaign involved assessing the RCS of a 6U (30x20x10cm) CubeSat manufactured by Dstl, with support from QinetiQ Ltd UK. RCS measurements were taken in an indoor anechoic measurement chamber of both the Flight Model (FM) of the CubeSat as well as a representative Engineering Model (EM). Mono-static RCS data was collected across a 3-40GHz frequency range, and included changes to the CubeSat orientation and studies on physical variations such as component deployment in order to produce a comprehensive dataset of the satellite.

Sections 2-3 outline the procedures adopted to produce the CubeSat models and conduct RCS measurements to safely capture a broad suite of data. An EM was produced to allow for an extended testing campaign that captured a range of orientations and configurations while minimizing risks to the Flight Model. Subsequent sections discuss the results collected, exploring how the FM and EM results compare as well as the impact to the RCS of the configuration changes. Finally, the future work is discussed, including plans to measure the CubeSat again on-orbit once launched and how interested parties may get involved in supporting this effort.

2. CUBESAT MODEL PRODUCTION

To allow for a thorough RCS measurement campaign that produced valuable data without exposing the FM to unnecessary risk, a representative model (dubbed the Engineering Model, EM) was produced. The CubeSat FM was developed within Dstl as an S&T exercise initially unrelated to SDA RCS research activities but, upon discussions with the mission team, it was agreed that it could be used as a measurement target of opportunity; so long as precautions were taken to minimize the risk of damage or exposure to dust or debris that could otherwise impede mission performance following launch. Both the CubeSat FM and EM were produced from Commercial of the Shelf (COTS) parts as the most cost-effective approach, omitting internal components that would be shielded from view by the external features and therefore have a reduced contribution to the RCS.

To ensure validity of the EM data, a subset of measurements were first conducted on the FM and repeated directly on the EM for comparison. Several safety precautions were taken for the FM measurements and were repeated on the EM for consistency. Further measurements on the EM were taken using a more flexible approach, reducing the restrictions for improved accuracy.

The structure and antennas were provided as genuine FM parts and spares for the duration of the RCS measurements; the mounting plates were produced to the same specification as those found on the FM and solar panels were sourced to provide as close a match to the FM as possible. As the antennas were disconnected from any internal components, they were attached to a matched load to replicate the installed antenna performance.

To reduce the cost and complexity of producing the EM, the Magnetometer, Propulsion Thruster and some Raspberry Pi Cameras were 3D printed using CAD supplied with their FM counterparts. These parts were produced in-house and subsequently prepared for RCS testing by first priming and then coating in a Copper Screening Compound that mimicked the material properties of a metal part. This preparation process resulted in the replica having a highly conductive outer layer that is able to provide a similar response to the measurement radar as the genuine FM part. This is a simplified approach to component replication: an assumption was made that the small and complex features of the genuine parts would have a negligible impact on the comparatively large RCS of the whole CubeSat, and therefore reducing the component to a metal representation would not have a significantly detrimental impact on the results.

This assumption is most robust at lower frequencies where the parts in question are much smaller compared to the size of the wavelength. The Magnetometer replica is approximately 82mm x 17mm x 8mm and the Camera replicas are approximately 42mm x 30mm x 18mm. The Thruster is a larger component however as it is primarily housed in a smooth metal box, the same assumption limitations are less prevalent, with the exception of the small emitting element that is approximately 28mm x 20mm x 5mm. At 3GHz the wavelength is 100mm, meaning the components in their entirety are smaller than a single wavelength; therefore smaller details of the components are all closer together than a single wavelength, rendering them effectively indistinguishable from the component as a whole. However at 40GHz the wavelength is 7mm, meaning at this frequency the components are several wavelengths long and smaller details on the components could have a separation of multiple wavelengths. Therefore these smaller features could contribute to the RCS at higher frequencies independently above the overall, simplified shape of the component represented by the replica.

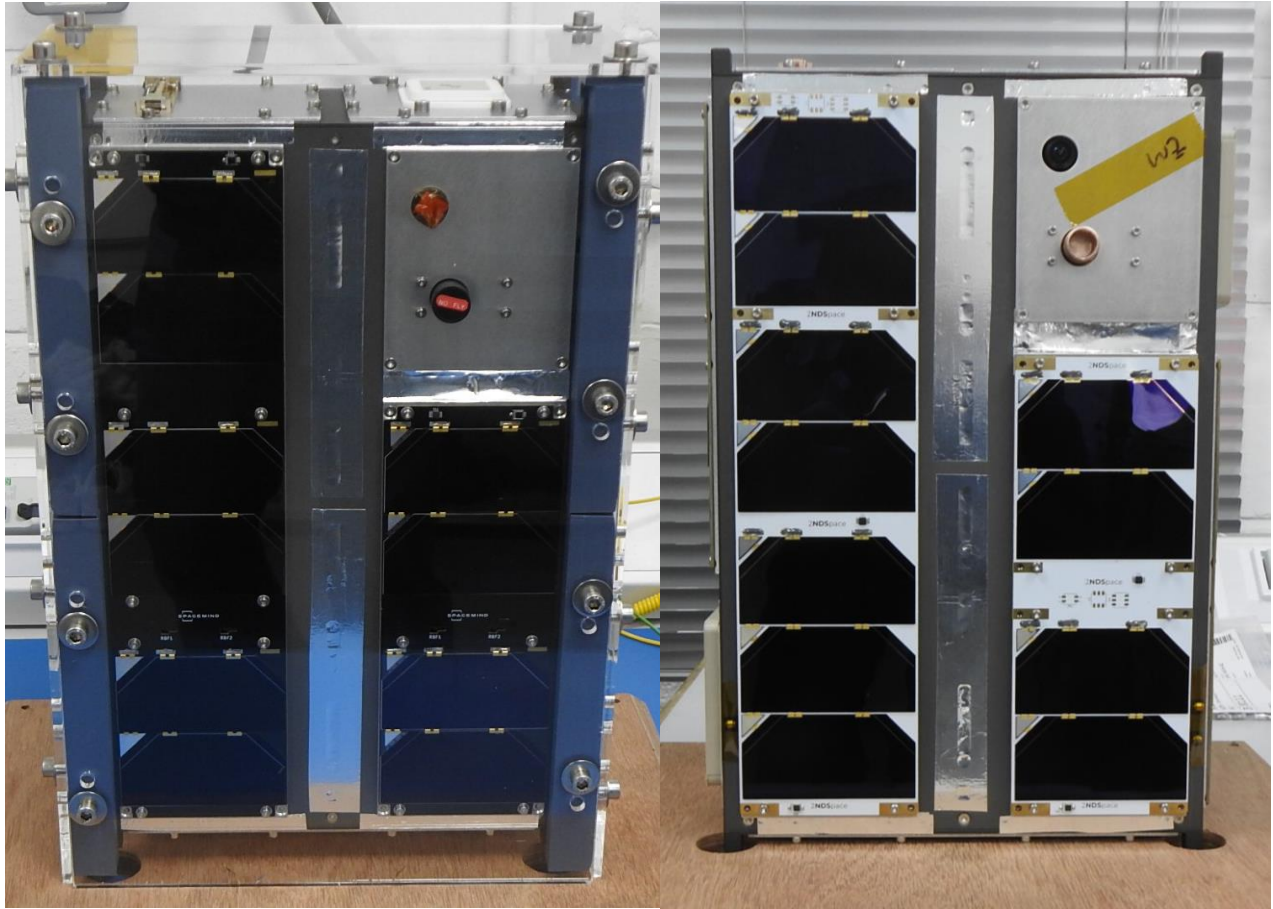


Fig. 1: Photographs showing the CubeSat FM, in a protective case and with camera lens covers (Left), and EM (Right).

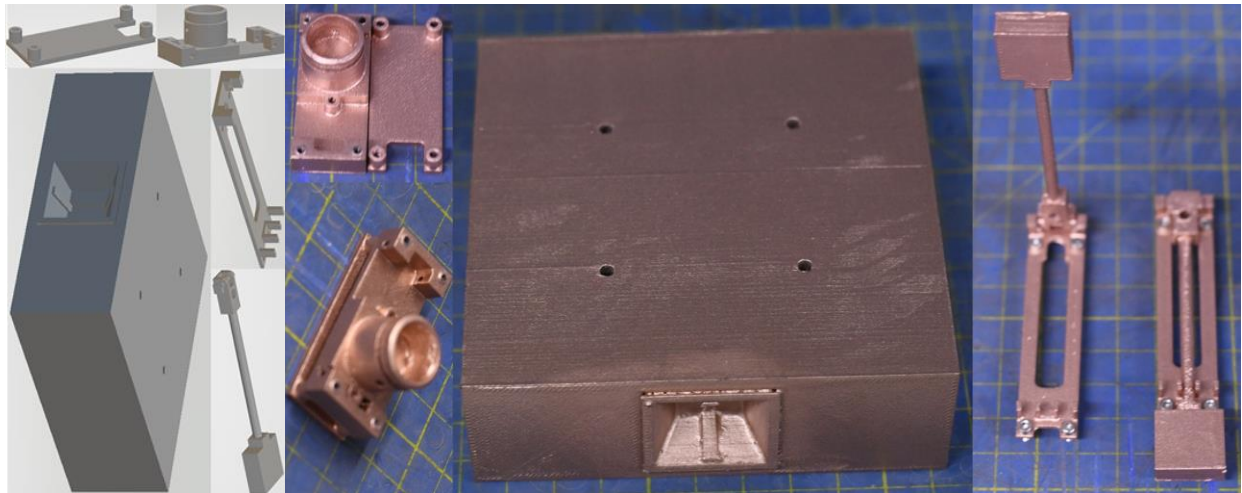


Fig. 2: Images showing CAD of the replica Magnetometer, Thruster and Cameras prior to printing and the 3D printed parts coated in an electro-magnetic conducting paint to mimic the properties of metal.

Finally, to minimize the risk of the FM toppling during the measurement process, a bespoke wooden interface piece was designed to secure the FM on top of the cone in the measurement chamber. The materials and design were chosen following discussions with SMEs within QinetiQ UK to maximise stability while providing a minimal impact on the measured RCS. This interface included an insert that fitted inside the FM and occupied the space where the Thruster (removed for the FM measurements) is normally housed. The interface was then tied down, resulting in a secure and

stable measurement setup. The wooden interface and strings used slightly impacted the quality of the results, however this compromise was made to ensure the chances of damaging the FM were minimised. When the EM was brought in for measurements, the first run repeated this approach to allow for direct comparisons with the FM whilst subsequent measurements removed the wooden interface for maximum accuracy.



Fig. 3: Photograph of the wooden interface piece produced for safely securing the FM to the polystyrene column. Includes a vertical block that inserts into the FM and four holes for the corners of the FM to sit securely. Four small holes for affixing strings can also be seen in the corners of the interface.

3. RADAR CROSS-SECTION MEASUREMENT PROCEDURE

RCS is a measure of the power scattered in a given direction when a target is illuminated by an incident radar wave, denoted by σ and expressed as the cross-sectional area of a theoretical sphere that would return the same magnitude of power. As RCS values typically range from 10^{-5} m² to 10^6 m², they are typically expressed in a logarithmic scale with units of dBsm (decibels per square metre) [5].

An object's RCS is dependent on a number of factors including the aspect presented to the radar as well as both the frequency and polarisation of the transmitted waveform. Therefore, measurements are typically collected over a range of frequencies and aspects to build up a comprehensive picture of the object's RCS. Polarisation refers to the orientation of the electric field (E-field) component of the electro-magnetic wave with respect to ground; the most commonly defined polarisations are Linearly polarised, in both Horizontal (H-Pol), where the E-field is parallel to the ground, or Vertical (V-Pol) where the E-field perpendicular to the ground [6]. Within the RCS community, the most commonly measured polarisations are "co-polar" H-Pol and V-Pol, where the same polarisation is used on both Transmit (Tx) & Receive (Rx). SDA radars typically operate circularly polarised (where the E-field rotates through 360° as the wave propagates through space), or transmit in one polarisation while receiving both to account for Faraday rotation that causes a polarisation rotation along the direction of the propagation. For these CubeSat measurements, both H-Pol and V-Pol co-polar data was collected.

A preparation procedure was developed for measuring the FM in a manner that reduced the risk of damage or accumulation of dust and debris to the fragile solar panels. For the entire measurement window, only the team developing the CubeSat were authorised to handle the FM in protective clothing. Alongside this, the FM was both transported and held in a custom-made protective case whenever not being actively measured.

As satellites are typically constructed in clean room environments with anti-static protections in place, the CubeSat development team brought some of these elements into the preparation room outside of the measurement chamber. The preparation room was cleaned and cleared of any unnecessary clutter and left undisturbed for several days ahead of the measurements. On the day of the measurements, the CubeSat development team set out anti-static mats and wore anti-static wristbands along with lab coats, gloves and hair nets and followed their established handling procedure for unpacking the FM and preparing it for measurement.



Fig. 4: Photographs showing the CubeSats in the measurement preparation room with the FM (left) in a protective case on an anti-static mat, and the EM set up (right) including the solar panel case, without these safety precautions.

RCS measurements conducted inside of an anechoic chamber routinely take place with the target placed on top of a tall column constructed from polystyrene in order to position the target in as close to a free-space region within the chamber as possible. Polystyrene is chosen for its structural properties and minimal RCS contribution, due to being 95% comprised of air. This column is then rotated through 360° to expose the full azimuth extent of the target to a transmitting measurement radar mounted within the chamber. A co-located receiver then detects the energy that is scattered back from the target and uses this to calculate the target's RCS. As the receiver collects all the energy returned from the chamber - including not only the target, but also the walls, polystyrene column, and in this case the wooden interface - it is important that efforts are undertaken to minimise the energy returned from these features. Some of these efforts can be seen in Fig. 5 and include the shaping of the polystyrene column and sides of the wooden interface, as well as the inclusion of Radar Absorbing Material (RAM) pyramids lining the chamber, all intended to either absorb incident energy or else direct it away from the receiver.



Fig. 5: Photographs showing the measurement chamber complete with RAM pyramids and antenna window at the end; the polystyrene column and the CubeSat team installing the FM onto the column.

Further efforts to reduce the impact of the background on the measurements include making a measurement of the chamber without the target installed and then subtracting this from the measurements of the target. However, as even small changes can affect the background return, including the slight disturbances of someone entering and exiting the chamber, multiple background measurements were required along the course of the measurement campaign. A calibration process is also undertaken to relate the power in the receiver to RCS and set the measurement phase reference, using a metal sphere of known RCS in place of the target.

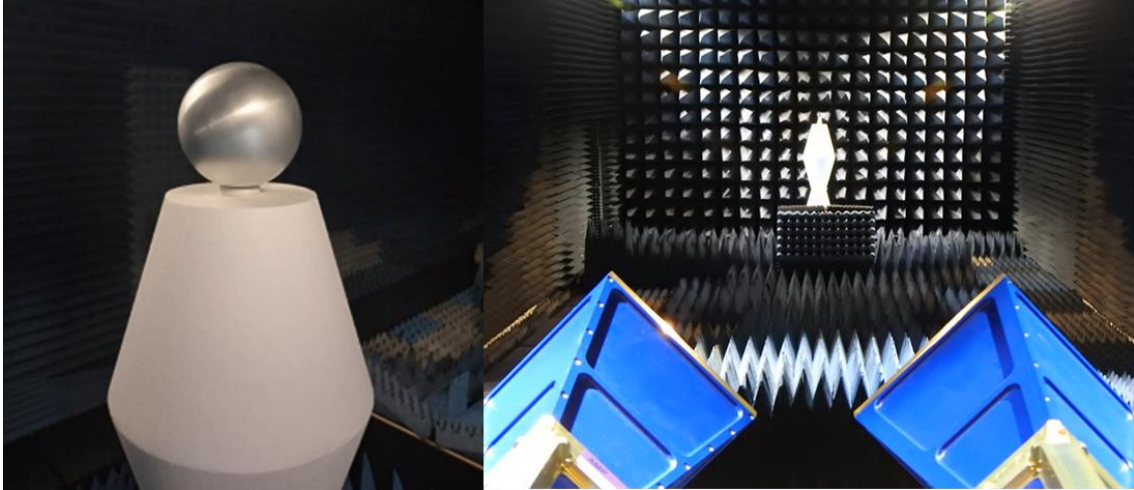


Fig. 6: Photograph of the calibration sphere used in RCS measurements. Right image shows the sphere in the chamber as seen from the measurement antennas.

The RCS measurements were taken at a number of frequencies across multiple bands, detailed below:

- 3-8GHz
- 7-18GHz
- 26-40GHz

A comprehensive test plan was developed in collaboration with the operators of the anechoic chamber, QinetiQ UK, with a focus on understanding the RCS-dominant features on the CubeSat as well as the impact of any variations to the RCS. As seen in Table 1, measurements were undertaken with the CubeSat in a number of configurations and orientations. Fig. 7 explains the CubeSat orientation conventions adopted for the measurement campaign, with each face of the CubeSat assigned a number to allow for ease of repeatability.

Table 1: Table showing the various configurations and orientations of the CubeSat that were measured.

CubeSat Configuration	CubeSat Orientations	Elevations
FM	A	0°
Wooden Interface (EM Repeat of FM measurements)	A	0°
Magnetometer Stowed (Also the EM Repeat without interface)	A, B	0° & 5° Conical A & B
Magnetometer Deployed (EM)	A, B, C	0° A, B & C, 5° Conical & 15° Great Circle A & B
Solar Panel Removed (Replaced with metal foil) (EM)	A	0°

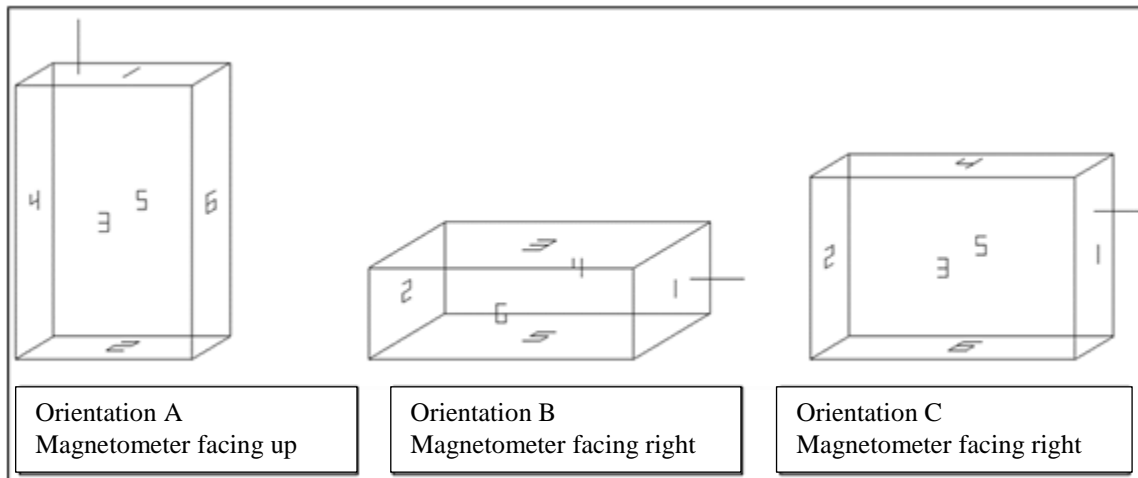


Fig. 7: Diagram demonstrating the orientation convention adopted for the CubeSat RCS measurements. These diagrams represent 0° azimuth for that orientation with the measurement radar located to the right.



Fig. 8: Photographs showing the five CubeSat configurations measured. From Left to Right: FM, EM (FM set up), EM Magnetometer Stowed, EM Magnetometer Deployed (on 15° Great Circle Cut wedge), EM Solar Panel replaced.

The measurements conducted on the FM and EM with the interface piece were limited to single orientation (A) and elevation (0°) as this offered maximum stability and minimum risk to the FM. For the measurements made without the interface, other orientations and elevations could be measured. In order to achieve measurements at different elevations, two methods were employed. The first method involves tilting the polystyrene column upon which the CubeSat is mounted, resulting in a shift of the angle of rotation away from that being perpendicular to the measurement radar. The second method involves placing a wedge of polystyrene cut to the desired elevation angle onto the column and then placing the CubeSat onto this for measuring, pitching the CubeSat but maintaining the perpendicular angle of rotation.

The measurements obtained from these methods for altering elevation angles are referred to as Conical and Great Circle cuts respectively. Conical cuts measure a constant angle with respect to the axis of rotation, sweeping out a conical area, while Great Circle cuts measure an angled circular cut through the target orientation [7]. This is because when the whole column is tilted for a Conical cut the CubeSat remains aligned with the axis of rotation, but when only the CubeSat is tilted for a Great Circle cut it is now offset from the axis of rotation. A diagram showing how the CubeSat was mounted for the measurement methods can be seen below in Fig. 9. Once the measurement data is collected, RCS can be post-processed and displayed in a number of ways for subsequent analysis, with some commonly used methods listed below:

- **RCS vs Azimuth Plots** – These plots show how the RCS varies with azimuth for a single frequency and elevation. They are useful for showing the signature variation and regions of both high and low signature for that specific aspect and frequency.
- **Inverse Synthetic Aperture Radar (ISAR) Images** – A 2D colour-map image showing data collected from a range in both frequency and azimuth. This image is generated by carrying out a 2D Fast-Fourier Transform (FFT) on the data and it can be used to identify sources of scatter on a target.
- **Frequency Profile Plots** – These plots show how the RCS varies with both azimuth and frequency, which can be used to identify frequency dependent regions of scatter on a platform.

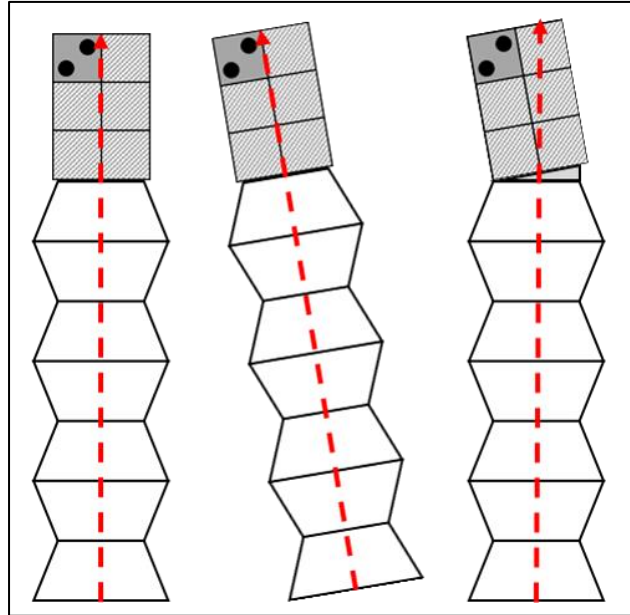


Fig. 9: Diagram showing the three methods adopted for measuring the CubeSat. Left: 0° elevation. Middle: 5° Conical cut method. Right: 15° Great Circle cut method. Red arrows indicate the axis of rotation.

4. RESULTS DISCUSSION

A selection of spot frequencies within the frequency bands collected are typically extracted and displayed in RCS vs Azimuth graphs for ease of analysis. Fig. 10 shows how the RCS of the CubeSat differs between the FM and EM runs with the same measurement parameters. The impact of the wooden interface is most visible around 0° azimuth, where the RCS of both the FM and EM are approximately 1dB higher than the EM run without the interface. Away from this aspect (and $\pm 180^\circ$) the impact of the interface on the measured RCS is minimised. This is possibly due to the shaping of the interface piece directing more energy away from the receiver at these aspects or the CubeSat RCS being high enough (especially at $\pm 90^\circ$) to obscure the contribution from the interface.

There are other slight regions of disagreement between the FM and EM runs; however, overall the RCS of the three CubeSat configurations follow the same trends, with both EM RCS being on average 1dB lower than the FM at this frequency. It can be seen that although the CubeSat appears visually symmetrical, there are slight variations in the magnitudes of RCS from each side. This is most apparent when comparing the peak RCS values around both 0° and $\pm 180^\circ$, where 0° is approximately 1-2dB lower than $\pm 180^\circ$ over a 5° window across these regions. Subtle differences on either side including slight flexing of the solar panel or the exact alignment of the undulations of the metal tape could be a cause of the observed differences in RCS, with these variations in particular being difficult to identify and account for.

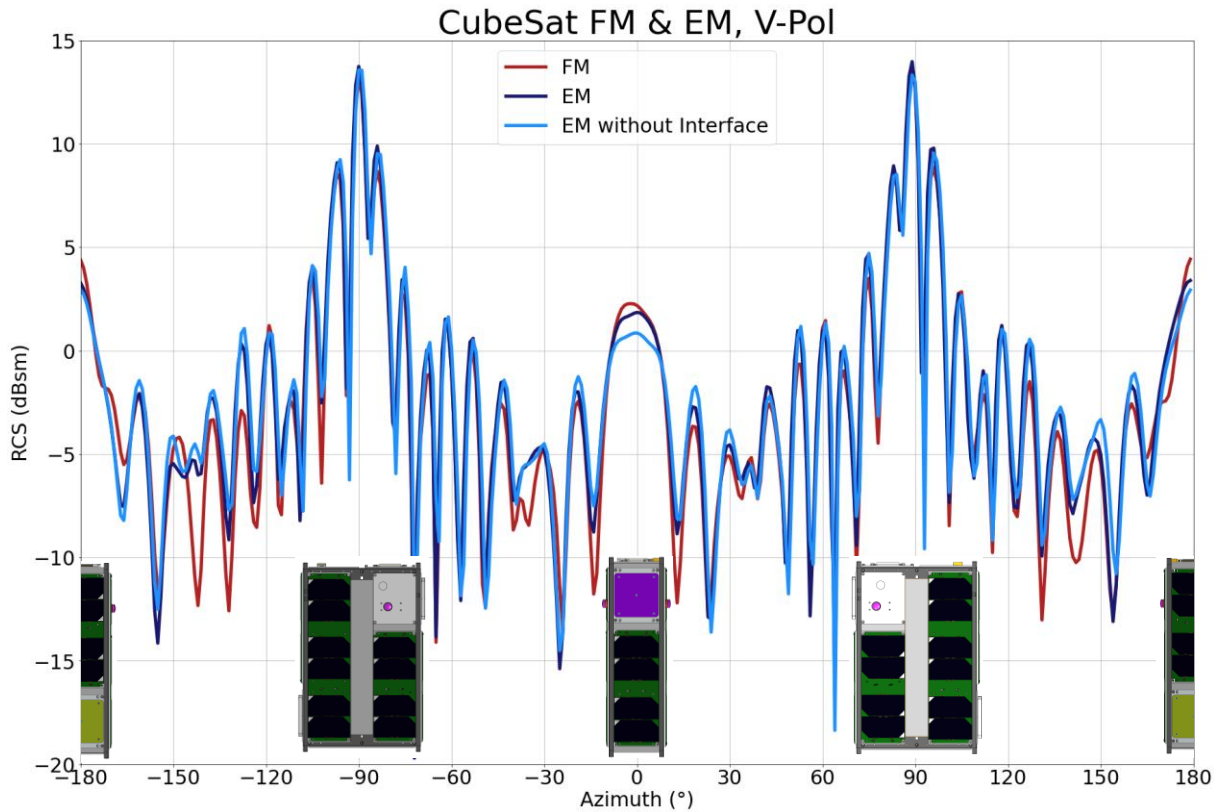


Fig. 10: RCS vs Azimuth graph showing how the RCS of the CubeSat FM & EM varies with azimuth in Orientation A. Images of the CubeSat are included to show how the CubeSat is presented to the radar at that point.

ISAR images are another useful tool for identifying the driving forces behind observed differences in RCS, and can show when something has changed on a target even if the impact of that change on whole target RCS is minimal. They can be viewed as a “top-down” image of the target, with the radar illuminating from the bottom of the image and the regions contributing to RCS (also known as the “scatterers”) represented in colour. As the radar wave is incident on the front face of the CubeSat, this returns the largest amount of energy to the receiver, with limited energy being scattered from any other region. In Fig. 11, the exposed faces of the CubeSat can be easily identified, with the slight protrusions of the Antenna and Solar Panels from the main structure being visible in the images.

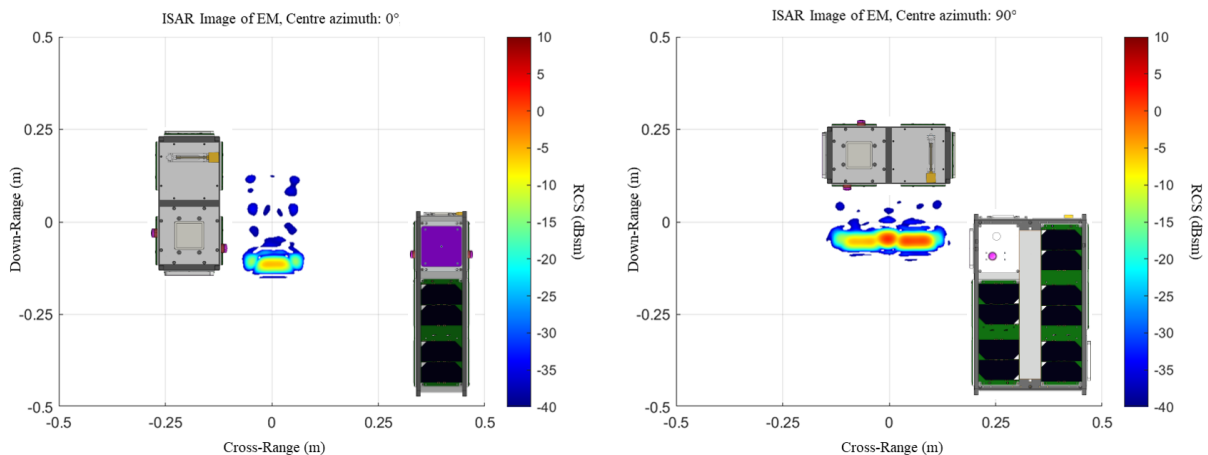


Fig. 11: ISAR images showing the dominant RCS features on the CubeSat at two azimuth points. CubeSat images show both a top down and radar-facing view (bottom right) corresponding to its position for that measurement. Both measurements took place with the CubeSat in Orientation A.

As frequency increases the RCS becomes more sensitive to small variations in the target, with smaller features and slight changes in aspect having a more significant impact. This can be seen in Fig. 12, where the lower frequency RCS changes much more gradually with azimuth than the higher frequency measurements. Another interesting feature is the double peak seen in the Mid Frequency data around 0° and $\pm 180^\circ$, where both High and Low Frequency measurements only record a single peak in the data at these aspects. This indicates a frequency-dependent response from the CubeSat at this azimuth. This may be due to interactions between the solar cells or within the antenna structure.

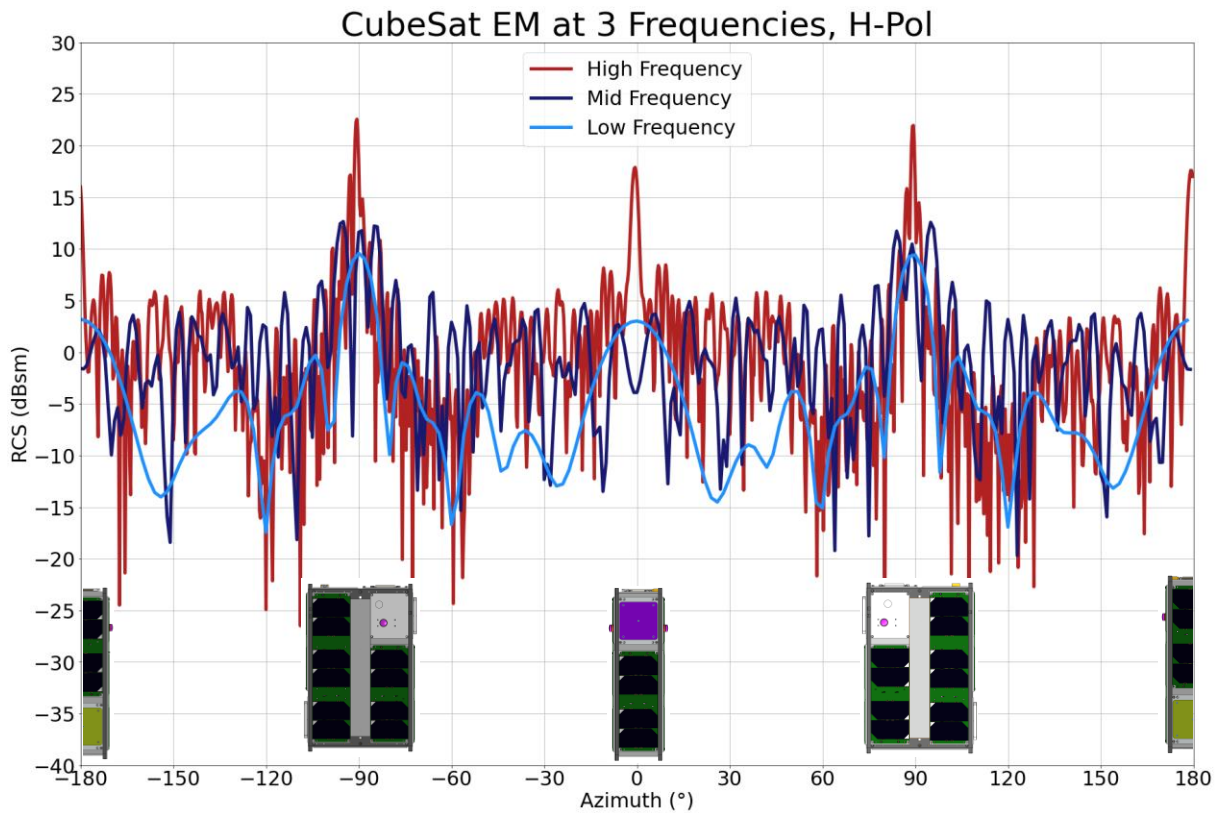


Fig. 12: RCS vs Azimuth graph showing the RCS of the EM at three frequencies in orientation A. Images of the CubeSat are included to show how the CubeSat is presented to the radar at that aspect.

As previous graphs demonstrate, the CubeSat RCS is highly dependent on the aspect presented to the radar. Measuring how RCS varies with elevation is therefore another important part of capturing the whole signature of a target. Fig. 13 shows how relatively small elevation changes can have a large impact in the overall RCS levels recorded for that azimuth sweep, with the RCS at both 5° and 15° elevation being on average 16dB and 18dB lower respectively than at 0° . It is worth noting that measurement process for the 15° Great Circle cut meant that at $\pm 90^\circ$ the CubeSat elevation was effectively 0° at that aspect, resulting in the peak responses at these aspects being very similar to the 0° measurements.

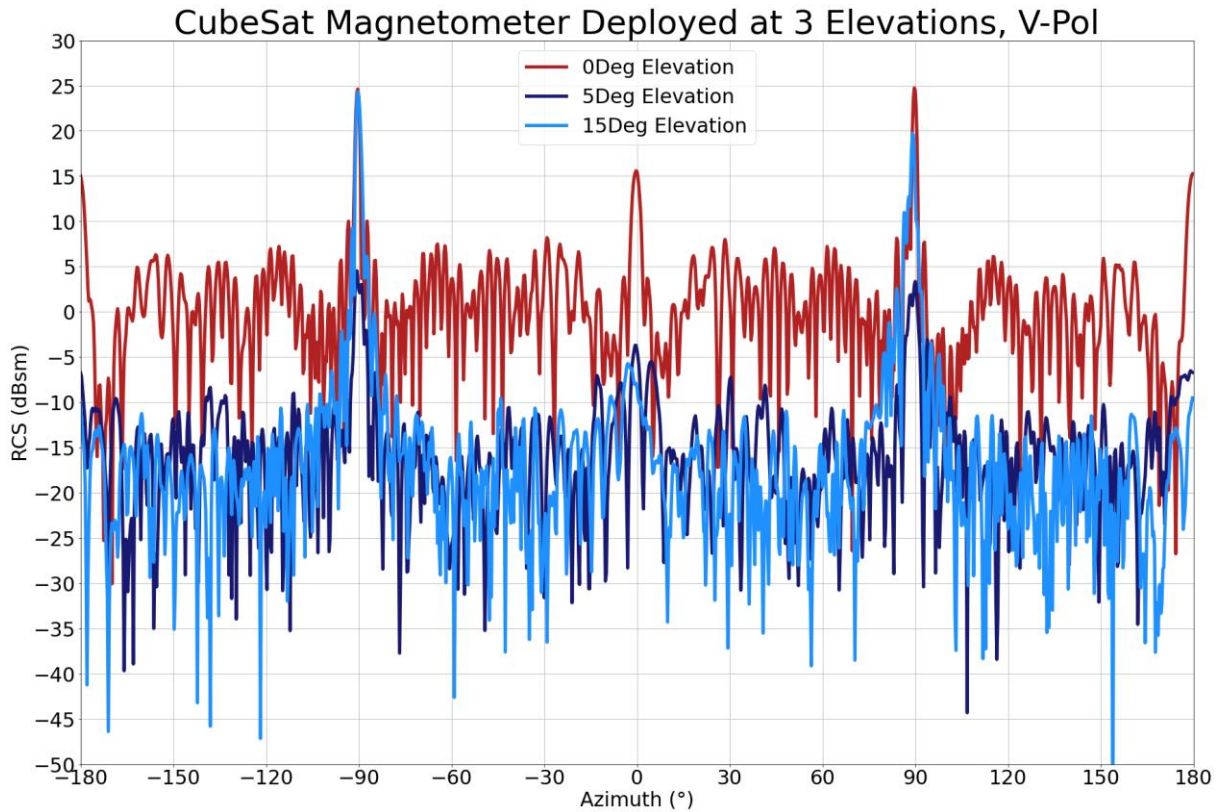


Fig. 13: RCS vs Azimuth graph showing the EM RCS with the Magnetometer deployed at 3 elevation angles. CubeSat images included to provide an indication of the elevations measured.

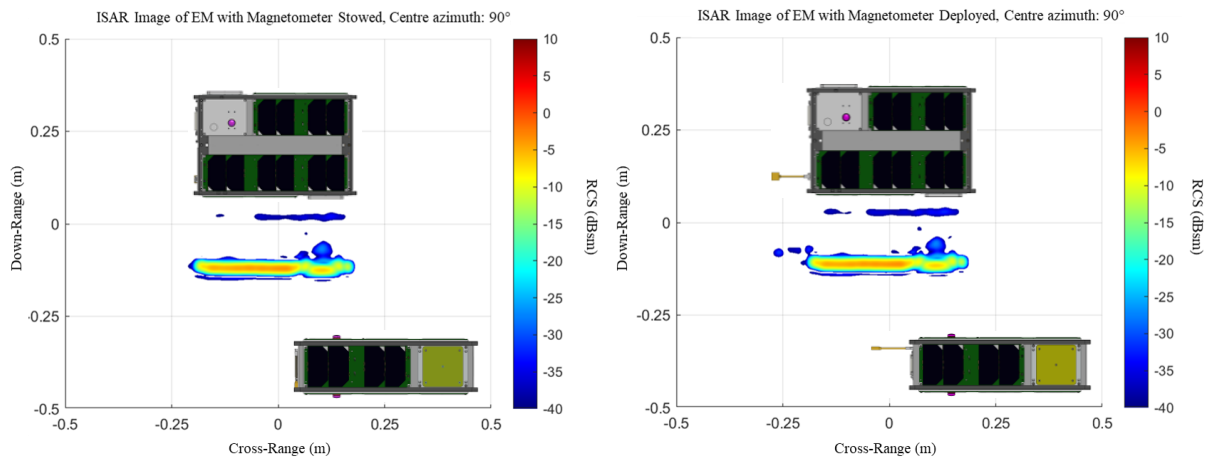


Fig. 14: ISAR Images showing the CubeSat EM measured at the same aspect and frequency, with the Magnetometer in the Stowed and Deployed positions. CubeSat images show both a top down and radar-facing view (bottom right) corresponding to its position for that measurement. Both measurements took place with the CubeSat in Orientation B.

Fig. 14 shows two ISAR images where the only change is the deployment of the Magnetometer replica. This feature is easily identifiable by the ISAR image as an extra source of scatter on the image resembling the Magnetometer, demonstrating the ease of which feature variation can be identified with ISAR imagery. When comparing with the graph in Fig. 15 that shows the RCS measured at a spot frequency, there is a negligible change in RCS between the two configurations across the azimuth sweep. This component deployment would therefore be very difficult to identify if observing the CubeSat with a radar at this single frequency instead of utilising ISAR imagery. Fig. 16 shows additional ISAR imagery where further CubeSat features can be identified, including the Cameras and GPS antenna.

CubeSat Magnetometer Stowed vs Deployed, H-Pol

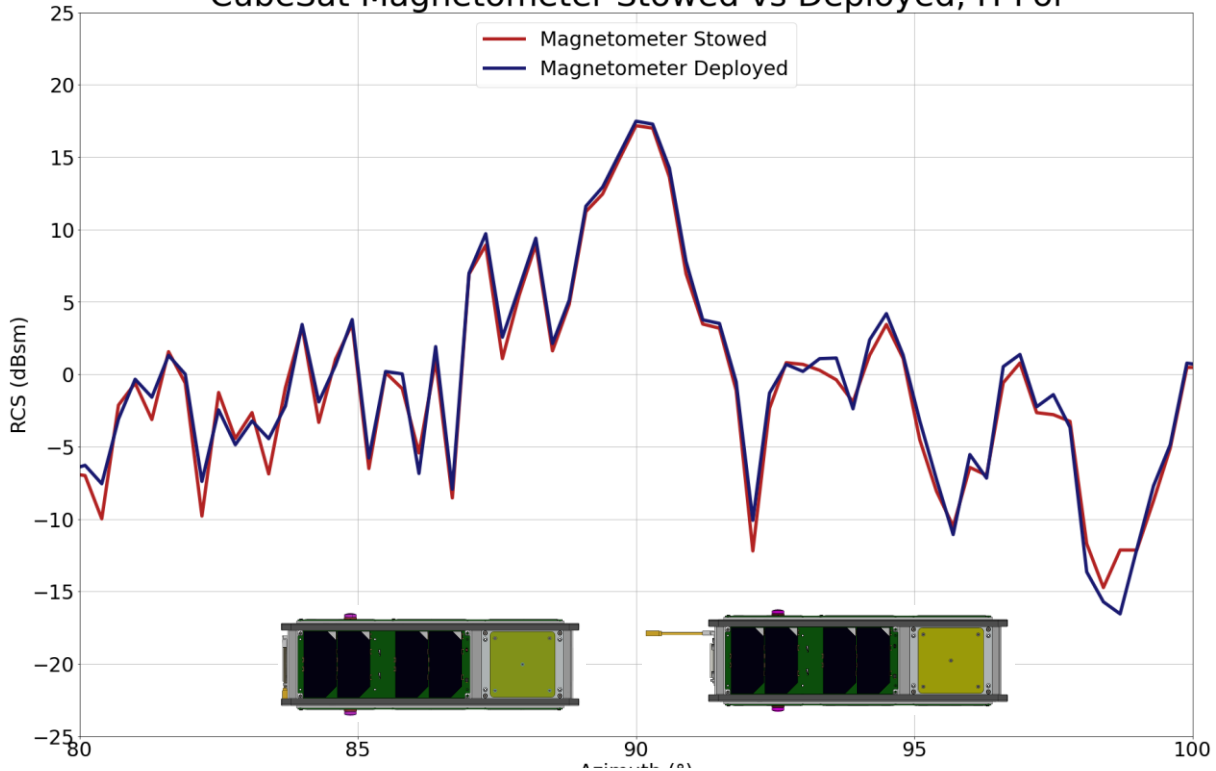


Fig. 15: Graph showing how the RCS of the CubeSat changes over 80-100° Azimuth with the Magnetometer in the Stowed and Deployed configurations. CubeSat images show the position for that measurement. Both measurements took place with the CubeSat in Orientation B.

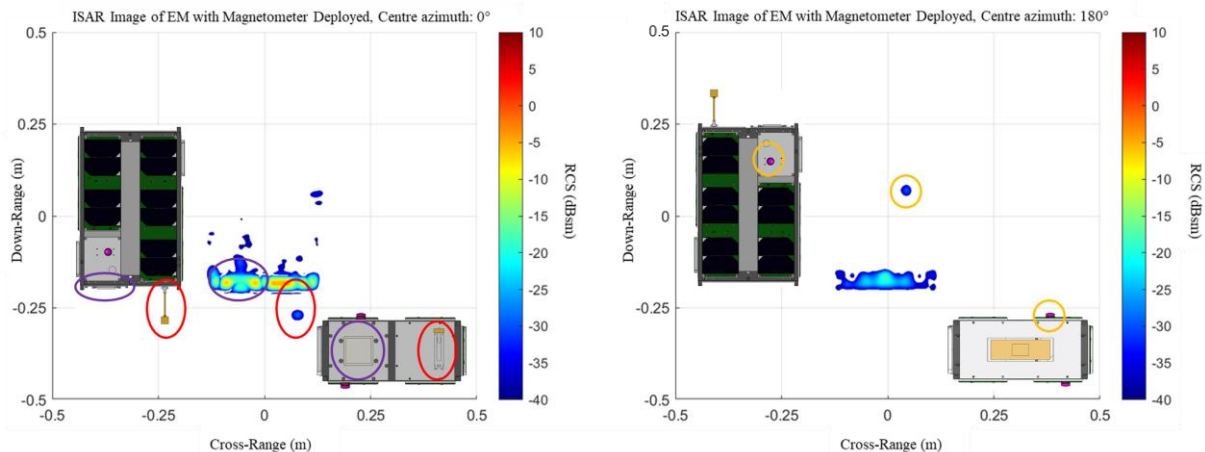


Fig. 16: ISAR images showing the CubeSat EM with multiple features identifiable. CubeSat images show both a top down and radar-facing view (bottom right) corresponding to its position for that measurement. Both measurements took place with the CubeSat in Orientation B, with the right ISAR image also at 15° elevation.

Another variation study conducted was removing a solar panel from one side of the CubeSat and replacing it with metal tape to assess if a satellite side with a solar panel had a measurably different RCS than one covered with a thin, non-uniform metal layer (similar to Multi-layer Insulation, or MLI). The metal tape was able to flex and bend slightly into access spaces within the CubeSat and therefore did not produce a completely flat surface. The effect of this can be seen most around 0° in Fig. 17 where while the peak response is lowered by 2.6-2.9dB compared to the two EM runs containing the solar panel, it is also broader, meaning the scatter from the taped region is less specular than the same side measured with a solar panel.

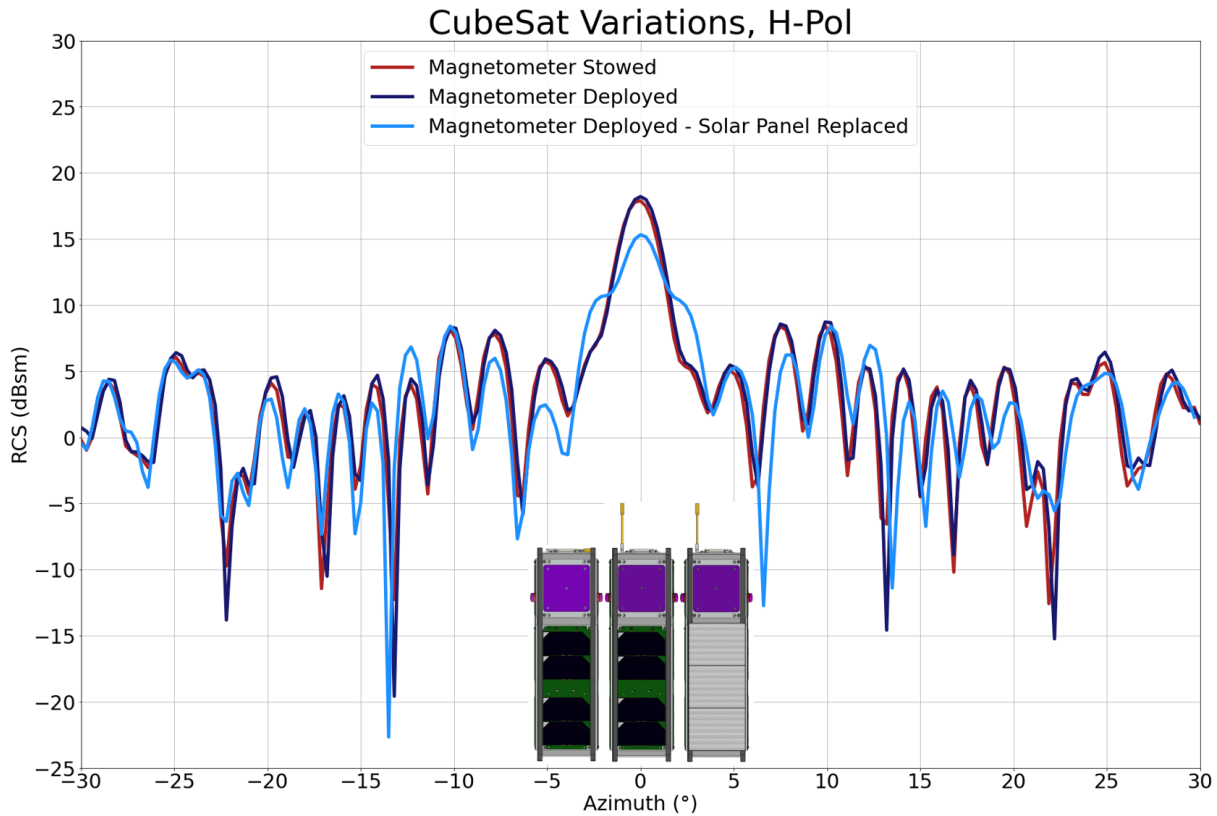


Fig. 17: RCS vs azimuth graph showing the effect on RCS of replacing a Solar Panel with metal tape. All measurements took place with the CubeSat in Orientation A.

When comparing the ISAR images in Fig. 18, there is a noticeable change in the front-face response where the solar panel was removed and the metal tape applied. As the return from the tape is less dominant, the responses from the corners of the CubeSat structure become visible. In the V-Pol ISAR images, the taped CubeSat also shows more of a response that seems to originate from inside the CubeSat. This is possibly the result of imperfect placing of the tape allowing some energy into the CubeSat, or alternatively there could be additional interactions between the radar wave and the CubeSat exterior that take longer to return back to the receiver, resulting in the response appearing inside the CubeSat structure.

Another feature of note in the H-Pol ISAR images is the two bright regions that can be identified in both configurations and appear to originate further back on the CubeSat. This is possibly caused by the discontinuity in the CubeSat surface in the centre of the faces between the solar panels. The reason it does not appear in the V-Pol images is related to the behaviour of electro-magnetic waves. Electro-magnetic waves are able to couple to and travel along conducting surfaces which are perpendicular to the polarisation of the wave.

As the CubeSat was in Orientation A, the H-Pol wave is able to couple with and travel along the vertically oriented faces, with the disruption of the solar panel edge resulting in scatter back to the receiver. This interaction does not occur when the surface is parallel to the polarisation of the wave as there is no direct contact between the electrical component of the wave and the surface, so it is therefore not visible in the corresponding V-Pol images.

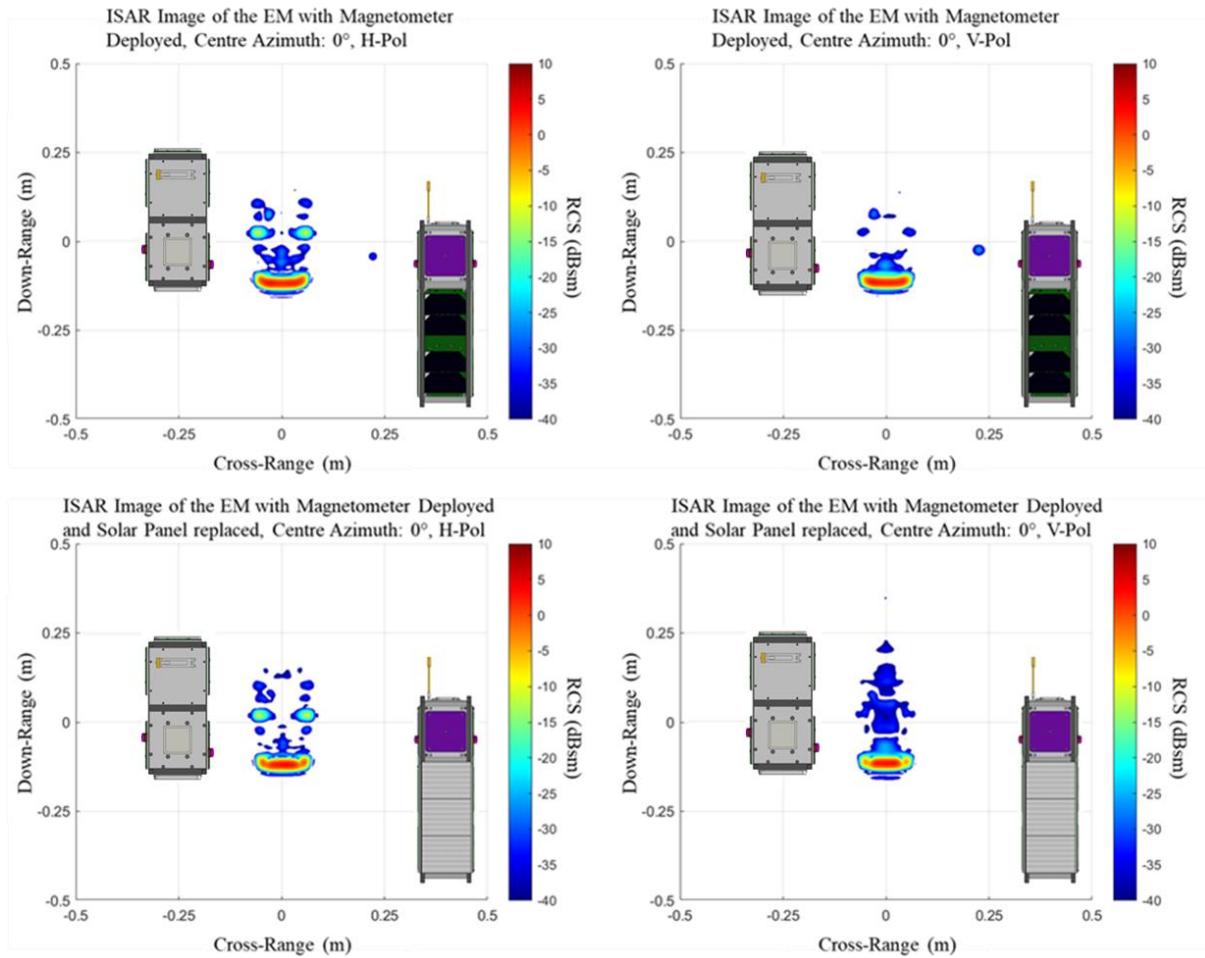


Fig. 18: A collection of ISAR images showing the CubeSat EM with the Magnetometer deployed and the Solar Panel replaced with metal tape. Both H-Pol and V-Pol ISAR images are shown. All measurements took place with the CubeSat in Orientation A. CubeSat images show both a top down and radar-facing view (bottom right) corresponding to its position for that measurement.

5. CONCLUSIONS AND FUTURE WORK

Through this measurement campaign, a comprehensive suite of measurements was conducted on a CubeSat FM and EM, characterising the signature across a broad range of frequencies, orientations and elevations. Multiple configurations of the CubeSat were also measured, including the deployment of a Magnetometer replica and replacing a solar panel with metal tape to mimic non-uniform metallic surfaces such as MLI.

A measurement process was developed to allow for safe and repeatable RCS measurements to be conducted on the CubeSat FM and again repeated on the EM. This process included ensuring that disturbance of the anechoic measurement chamber was kept to the absolute minimum required, with several days of inaction between prepping the chamber and conducting the measurements in order to reduce the presence of airborne particles. The FM was also subject to strict handling constraints, with designated personnel only permitted to handle the FM and a specially-designed protective case employed whenever the FM was not being actively measured; anti-static protections were also brought into the preparation chamber and protective clothing worn.

Background measurements were taken at multiple occasions during the campaign, where the CubeSat was removed from the chamber to characterise the response from the chamber structure. Alongside this a standardised calibration procedure was adopted in order to ensure the validity of the measurement data. This involved measuring metal spheres of a known RCS and subsequently using these results to calibrate the CubeSat data.


Analysis on the data collected showed it is possible to easily identify changes in the CubeSat configuration between measurements, with ISAR imagery especially useful in determining the position and size of any changes. The deployment of the Magnetometer has a negligible impact on the RCS when viewed in spot frequency Azimuth vs RCS graphs, making it very difficult to identify. However when viewing ISAR imagery that makes use of data from a range of frequencies, the scatter from the deployed Magnetometer becomes very easy to identify.

The impact on signature of replacing a rigid solar panel with a flexible metal tape to produce a non-uniform conducting surface was also assessed. This study showed that the irregularity of the tape produced a smaller but wider peak response in RCS as a result of less energy being directed back to receiver when the face was exactly aligned with the radar, but more energy returned when away from that angle. This also confirmed that the solar panels produce an RCS response similar to that of a flat metal plate, where a very strong return is seen when directly illuminating the face of the panel that quickly falls away when illuminating it from different angles.

The CubeSat's RCS was shown to be highly dependent on the aspect presented to the radar and the frequency of the illuminating radar. The RCS at lower frequencies was shown to change more gradually with aspect, while higher frequencies produced increasingly spiky RCS that changed rapidly with aspect. This is a result of the wavelength decreasing and therefore smaller features on the CubeSat having a greater impact on the RCS as they become larger and larger compared to the wavelength.

Future measurements are also planned within the anechoic chamber with the aim of expanding the frequency and aspect RCS collection of the CubeSat. Additionally, when the CubeSat is launched there will be efforts to observe and track it on-orbit, collecting in-situ validation data of the measurements and modelling work undertaken on the ground. Many of the measurements already collected will be replicated in space for direct comparison with the chamber measurements. This effort is open to interested parties to get involved in and there is an invitation extended from this work for collaboration on observing and tracking the CubeSat as a co-operative target of interest. There will be opportunities to collaborate on and help shape the measurement campaign and share in the results.

If this is of interest to you then please contact the author of this paper at: mmayne@dstl.gov.uk

© Crown copyright (2024), Dstl. This information is licensed under the Open Government Licence v3.0. To view this licence, visit <https://www.nationalarchives.gov.uk/doc/open-government-licence/> . Where we have identified any third party copyright information you will need to obtain permission from the copyright holders concerned. Any enquiries regarding this publication should be sent to: Dstl.

6. REFERENCES

- [1] T. Jennings-Bramly and J. Maxey, "An End-to-End Signal Processing Chain for Low Earth Orbit Inverse Synthetic Aperture Radar Space Object Imaging," in *Proceedings of the Advanced Maui Optical and Space Surveillance (AMOS) Technologies Conference*, 2023.
- [2] "Cross Government Space Domain Awareness (SDA) Requirements Publication," <http://www.gov.uk/government/publications/space-domain-awareness-requirements>, 2023.
- [3] E. Kerr, "UK SDA Requirements for a System of Systems in Support of the UK's SDA Strategy," in *Proceedings of the Advanced Maui Optical and Space Surveillance (AMOS) Technologies Conference*, 2023.
- [4] D. W. Hess, "Introduction to RCS Measurements," in *Antennas & Propagation Conference*, Loughborough, 2008.
- [5] E. F. Knott, M. T. Shaeffer and M. T. Tuley, "*Radar Cross Section, Second Edition*," SciTech Publishing Inc., 2004, p. 64.
- [6] B. Y. Toh, R. Cahill and V. F. Fusco, "Understanding and measuring circular polarization," *IEEE Transactions on Education*, vol. 46, no. 3, p. 314, 2003.
- [7] E. F. Knott, M. T. Shaeffer and M. T. Tuley, "*Radar Cross Section, Section Edition*," SciTech Publishing Inc., 2004, pp. 462-464.